Dynamic equilibrium under vibrations of H_2 liquid-vapor interface at various gravity levels

G. Gandikota,[1] D. Chatain,[1] T. Lyubimova,[2,3] and D. Beysens[1,4]
[1]*SBT, UMR-E CEA / UJF-Grenoble 1, INAC, Grenoble, F-38054, France*
[2]*Institute of Continuous Media Mechanics UB RAS, 1, Koroleva Strasse, 614013, Perm, Russia*
[3]*Perm State University, 15, Bukireva Strasse 614990, Perm, Russia*
[4]*CEA-ESEME, ESPCI-PMMH, 10, rue Vauquelin, 75005, France*
(Received 23 December 2013; revised manuscript received 10 March 2014; published 6 June 2014)

Horizontal vibration applied to the support of a simple pendulum can deviate from the equilibrium position of the pendulum to a nonvertical position. A similar phenomenon is expected when a liquid-vapor interface is subjected to strong horizontal vibration. Beyond a threshold value of vibrational velocity the interface should attain an equilibrium position at an angle to the initial horizontal position. In the present paper experimental investigation of this phenomenon is carried out in a magnetic levitation device to study the effect of the vibration parameters, gravity acceleration, and the liquid-vapor density on the interface position. The results compare well with the theoretical expression derived by Wolf [G. H. Wolf, Z. Phys. B **227**, 291 (1969)].

DOI: 10.1103/PhysRevE.89.063003 PACS number(s): 47.20.−k, 64.70.F−

I. INTRODUCTION AND BACKGROUND

A fluid interface interacts with vibration, giving rise to various interesting phenomena depending on the relative direction of the vibration and the interface. Vibration perpendicular to the interface can lead to a parametric instability (known as the Faraday wave instability [1–3]) whereas vibration parallel to the fluid interface can lead to the formation of frozen wave instability [4–7]. While the Faraday waves occur due to the parametric excitation of an interface, the frozen waves are caused by a shear-driven mechanism similar to the Kelvin-Helmholtz instability.

When subjected to vibration a fluid interface can share many similarities with that of simple mechanical systems under vibration. It is known that the vibrations are able to stabilize the equilibrium states which were unstable in the absence of vibrations and to create new equilibrium states. In a usual pendulum with a fixed suspension point, the only stable equilibrium position is the position with the bob below the suspension point. The inverted position where the mass is above the suspension point corresponds to an unstable equilibrium.

Kapitza considered the stability of a pendulum when the point of suspension was submitted to harmonic vibrations [8,9]. The stability properties of this system have been studied either by means of averaged equations (the effective potential method; see below) or by linearization around fixed points, which leads to the Mathieu equation. Kapitza analyzed the case of rapid oscillations with small amplitude (a) of the suspension point of a pendulum with length l_0, corresponding to $a \ll l_0$ and $\omega \gg \Omega$, with $\Omega \geqslant \sqrt{g_0/l_0}$ the eigenfrequency of pendulum oscillations (g_0 is the gravity field acceleration constant). He split the motion into fast and slow components and introduced an effective potential U_{eff} to describe the slow component. The stable equilibrium states of the pendulum correspond to the minima of U_{eff}.

To analyze the equilibria of the Kapitza pendulum, a periodic generalized force was introduced by Landau and Lifshitz [10] as the derivative of the Lagrangian with respect to the generalized coordinate, $f = \partial\mathcal{L}/\partial\varphi$ (φ is the angle between the pendulum and the vertical direction). For vertical vibrations of the suspension point the generalized force is $f = -ml_0a\omega^2\cos(\omega t)\sin\varphi$ and the effective potential takes the form

$$U_{\text{eff}} = mgl_0\left(-\cos\varphi + \frac{a\omega^2}{4gl_0}\sin^2\varphi\right), \tag{1}$$

where m is the pendulum mass. When $a\omega \geqslant \sqrt{2gl_0}$ the potential U_{eff} exhibits two minima. The first minimum corresponds to the vertical position of the bob below the suspension point ($\varphi = 0$); this state is always stable. The other minimum corresponds to an upper vertical position. This later position, unstable for a pendulum, thus becomes stable for the Kapitza pendulum. A physical explanation of the stability of the inverted pendulum position has been proposed in [11]: For rapid oscillations of the axis, a time averaged on the period gives rise to a nonzero torque that makes the upward position stable.

When the suspension point is vibrated horizontally, the generalized force becomes $f = -ml_0a\omega^2\cos(\omega t)\cos\varphi$ and the effective potential takes the form

$$U_{\text{eff}} = mgl_0\left(-\cos\varphi + \frac{a\omega^2}{4gl_0}\cos^2\varphi\right). \tag{2}$$

For $a\omega \leqslant \sqrt{2gl_0}$, the state with vertical position of the bob below the suspension point ($\alpha = 0$) is stable. For $a\omega \geqslant \sqrt{2gl_0}$, the equilibrium state corresponds to the pendulum inclined with angle φ such as

$$\cos\varphi = \frac{2gl_0}{a^2\omega^2}. \tag{3}$$

As shown by Wolf [5] a similar behavior can be observed in the case of an interface between two fluids under a gravity field, in a rectangular cavity subjected to small-amplitude, high-frequency vibrations. The width of the vessel, l, is assumed to be much smaller than the depth of the two fluids. Wolf introduced a time-averaged effective potential U_{eff} for a single particle of a mass m in a rapidly oscillating field with $\omega \gg \Omega$, in the same way as it was made in [10] for the Kapitza pendulum. For horizontal vibrations of the container, the angle φ in the formula (2) for the effective potential should be taken as the angle between the equilibrium position of the interface without vibrations (which is horizontal) and its position under

vibrations (which is inclined). Wolf introduces the angle α between the vertical upward position and interface position under vibrations (inclined position). One should thus substitute $\varphi = \frac{\pi}{2} - \alpha$ in formula (2) for U_{eff}, which becomes

$$U_{\text{eff}} = mgl_0\left(-\sin\alpha + \frac{a\omega^2}{4gl_0}\sin^2\alpha\right). \tag{4}$$

The equilibrium positions of the fluid interface correspond to the minima of this potential, given by

$$\sin\alpha = \frac{2gl_0}{a^2\omega^2}. \tag{5}$$

The formulas (1) and (2) for the effective potential U_{eff} of the Kapitza pendulum contain the eigenfrequency of the pendulum oscillation $\Omega = \sqrt{g/l_0}$. Assuming that the formula for the effective potential can be generalized for the case of a fluid interface, Wolf uses for Ω the formula for the frequency of waves at the interface of two thick layers of inviscid fluids under a gravity field and in the absence of capillary effects:

$$\Omega^2 = kg\frac{\rho_l - \rho_v}{\rho_l + \rho_v}, \tag{6}$$

where k is the wave number. Then Eq. (5) can be rewritten as

$$\sin\alpha = \frac{2g^2}{a^2\omega^2\Omega^2} = \frac{gL}{\pi a^2\omega^2}\frac{\rho_l + \rho_v}{\rho_l - \rho_v}, \tag{7}$$

where $L = 2\pi/k$ is the wavelength of perturbations.

For the rectangular container of greater lateral width l, taking $L/2 = l$, Eq. (7) becomes

$$\sin\alpha = \frac{2gl}{\pi a^2\omega^2}\frac{\rho_l + \rho_v}{\rho_l - \rho_v}. \tag{8}$$

It follows from (8) that the angle α should grow with the increase of lateral width of the vessel. Note that for some values of vibration parameters, and density or gravity values, the expression (8) can give values larger than unity. It simply means that $\sin\alpha$ saturates to unity.

The present paper deals with the dynamic equilibration of a fluid interface when subjected to horizontal vibration. The problem has been surprisingly poorly investigated until now. Only two research articles related to this phenomenon could be found. Wolf [5] first reported the phenomenon when experimenting with aqueous solution of potassium iodide and oil. He observed that for large-amplitude, high frequency cases the interface indeed tilts towards a wall at an angle α to the vertical according to Eq. (8) that he derived. The experiments were carried out for a fixed value of aspect ratio ($h/l = 1$). Later, Lyubimov *et al.* formulated in [12] a variational principle for the determination of the free surface shape of a fluid subjected to the high-frequency horizontal vibrations. Numerical minimization of the corresponding functional has shown that the results obtained for different aspect ratios are qualitatively the same and that for the same vibration velocity amplitude ($a\omega$), α is larger for values of h/l much larger than 1.

The objective of the present paper is thus to investigate the above phenomenon when the density differences between liquid and vapor phases and the g levels are varied. Working with a fluid system involving a liquid layer surrounded by its own vapor near its critical point is indeed advantageous. Close to the critical point the physical properties of a fluid follow scaled universal power laws [13]. When the critical point is approached, various parameters such as the thermal expansion coefficient, isothermal compressibility, thermal conductivity, etc., diverge while properties such as surface tension, liquid-vapor density difference, capillary length, and coefficient of thermal diffusivity, etc., vanish. The fact that the capillary length goes to zero when approaching the critical point even with weak gravity fields makes capillary effects negligible. So just by heating or cooling the fluid (or in other words, by approaching or moving away from the liquid-vapor critical point) one can modify the properties of the liquid and vapor phases in a scaled way and thus study the interface for a variety of fluid conditions without having to change the fluid combination. Also, it is interesting to note that working close to the critical point decreases the density difference between the two fluids which, according to Eq. (8), leads to a magnification in the angle of the tilted interface under vibration. The effect of gravity is studied by changing the gravity level inside a small cell by using a magnetic levitator.

The present paper is organized as follows. Firstly, a brief description of the experimental setup used to carry out the experiments is given followed by the results of the experiments and comparison with theory. Lastly, some important conclusions drawn from the experiments are made.

II. EXPERIMENTAL SETUP

The experiments are carried out with H_2 as the working fluid using the cryogenic facility HYLDE (HYdrogen Levitation DEvice [14–16]). The HYLDE setup uses a 10 T magnetic field generated by a cylindrical superconducting coil. Hydrogen can be levitated near the upper end of the coil where is present a near-constant magnetogravitational potential field (product of magnetic field and its gradient) ($\approx 1000\,\text{T}^2\,\text{m}^{-1}$). The setup is shown schematically in Fig. 1(a). A superconducting coil made of Nb-Ti is dipped inside liquid helium at a temperature of 2.16 K and a pressure of 0.1 MPa inside the cryostat. The experimental cell is mounted inside another cryostat (the "anticryostat") maintained under a vacuum of less than 10^{-7} mbar. Endoscopes for a light source and a video camera are mounted inside the anticryostat as can be seen in Fig. 1. The positions of the endoscopes are independently adjustable. The experimental cell is vibrated using a motor-driven cam mechanism. The motor and cam assembly mounted on the top of the anticryostat [shown in Fig. 1(a)] is connected using a long shaft (not shown in the figure) to the vibration arm of the cell [shown in Fig. 1(b)]. The rotational motion of the motor is converted into a rocking motion of the shaft due to the cam assembly. The rocking motion of the shaft results in an oscillatory motion of the cell along a pivot shown in Fig. 1(b). The oscillation amplitude being very small, the net effect is equivalent to a horizontal vibration (see end of Sec. II for further details).

It has been demonstrated by Quettier *et al.* [16] that in the technique of magnetic levitation using a solenoid of cylindrical configuration, a total compensation of gravity can be obtained only at a single point. A residual gravity field is radially directed towards the center of the cell. The uniformity of the gravity field depends on the size of the cell. Using the setup

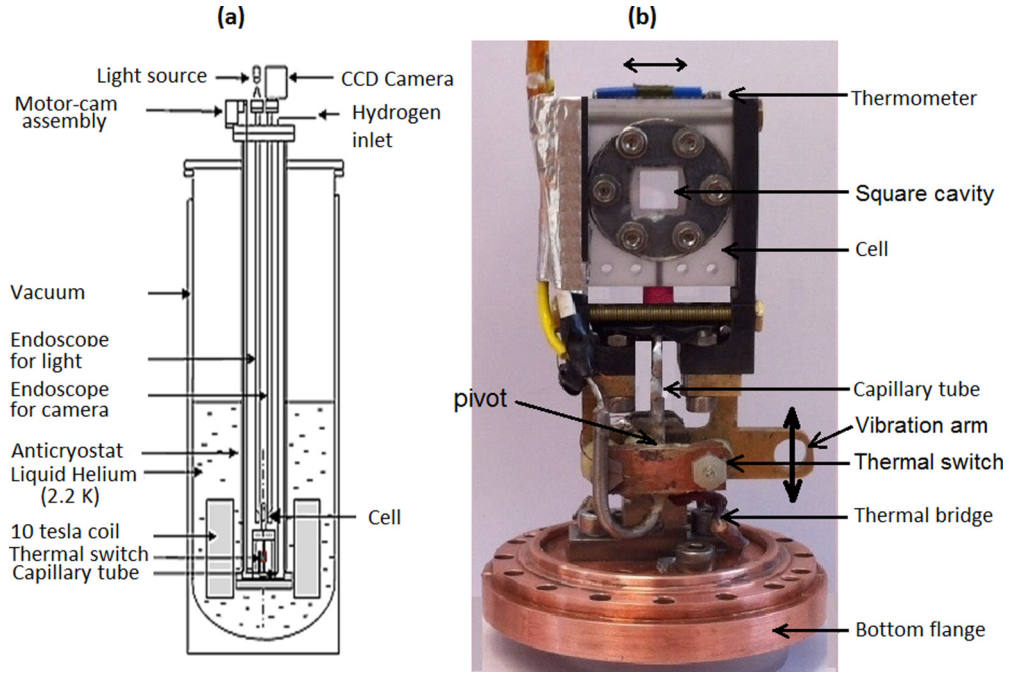

FIG. 1. (Color online) (a) Schematic diagram of the experimental setup HYLDE; (b) experimental cell of size 7 mm × 7 mm × 7 mm.

HYLDE a uniformity better than 1% and 2.5% can be achieved in cells of size 3 and 7 mm, respectively.

The experimental cell used [Fig. 1(b)] is a cubical cavity of side 7 mm, made of sapphire. The experiments are performed within 24 h after filling the cell with H_2 initially at room temperature. With the relaxation of H_2 spin polarization takes place slowly with a time constant of 50 h. The fluid is thus n-H_2, whose critical point is defined by: temperature T_c= 33.19 K, pressure p_c= 1.315 MPa, and density ρ_c= 30.11 kg m^{-3} [14]. Hydrogen is filled inside the cell at a density ρ within 0.2% of its critical density using a capillary tube of inner diameter 0.5 mm. To determine the critical density, the cell is filled (without gravity compensation) up to half its height at a temperature very close to the critical point (say 50 mK) and the meniscus is monitored for small temperature increase or decrease of the cell (50 mK on either side of the filling temperature). If the level of the meniscus does not change with temperature, it means that the cell is filled at its critical density.

This method of filling the cell at the critical density of the fluid is quite precise and the cell density is close to the critical density ρ_c, with an error of ±0.2% [17]. The capillary tube is fitted with a thermal switch, a small block of copper continuously cooled under the triple point of H_2, by conduction, by connecting it to the bottom of the anticryostat (which experiences 2.17 K temperature due to direct contact with helium inside the cryostat) and heated whenever required using a resistive heater. In the absence of heating the hydrogen inside the capillary tube freezes, thus closing the cell. To fill or empty the cell, the switch can be heated, thus melting solid H_2 inside the capillary tube.

The experimental cell is provided with thermal bridges, strands of copper wires connecting the bottom flange of the anticryostat, which is maintained at liquid helium temperature, and the cell. Resistive heaters in thermal contact with the cell are used to heat and control the temperature of the cell. Two thermometers are pasted on either side of the cell to monitor the temperature of the cell. The temperature control of the cell is achieved by using a standard PID (proportional, integral, differential) control system.

The cell is oscillated along a pivot with various frequencies (f = 10–50 Hz) and various amplitudes (a = 0.1–1 mm). It is estimated that for a frequency of 50 Hz and for maximum amplitude of 1 mm, the cell experiences an oscillation in the vertical direction of ±10 μm which is negligible compared to the amplitude of the horizontal vibration. Also, the resulting centripetal acceleration compares to the vibrational acceleration as a/R (where a is the amplitude of vibration and R is the distance of the cell from the pivot) which comes out to be of the order of 1/60. Thus the centrifugal force is negligibly small in the frequency and amplitude ranges considered and the vibration can be assumed to be in the horizontal direction.

III. RESULTS AND DISCUSSION

The experimental configuration is shown in Fig. 2. Hydrogen is filled inside a cubical cell of side 7 mm at its critical density. To carry out the experiments the cell is first maintained at a temperature slightly lower than the critical temperature T_c (say T_c − 100 mK) and then horizontal vibration is applied. The temperature of the cell is increased very slowly (20 mK min^{-1}) so that the fluid can be assumed to be under thermodynamic equilibrium at all temperatures. Experiments are conducted for various combinations of amplitudes (ranging from 0.2 to 0.8 mm) and frequencies (between 10 and 35 Hz). Various gravity levels, g = 0.18g_0,0.1g_0,0.05g_0,0.01g_0, and 0g_0 (g_0 is the gravitational acceleration), are obtained by adjusting the current intensity in the coil. The experimental results show no

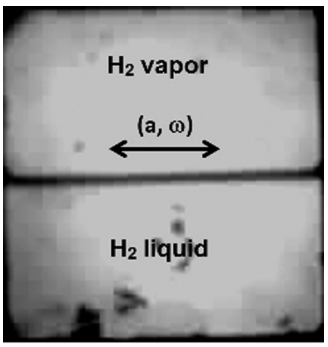

FIG. 2. Experimental configuration.

signs of hysteresis, meaning that pinning of the interface at the walls is negligible.

The images obtained from the experiments are analyzed using standard image processing software. Due to the fact that the interface oscillates in phase with vibration around its mean position, the interface looks fuzzy. Thus the measurements are made at the middle of the interface. A similar procedure is followed for all the measurements at all vibration levels. A measurement error of around ±5% may be expected in the angle measurements.

A. Determination of the fluid temperature

It is important to mention that the experiments have a serious limitation with respect to the measurement of the temperature. Since the thermometers fixed to the cell vibrate along with the cell inside an intense magnetic field, eddy currents are induced inside them and their electric cabling, provoking unwanted oscillations in the temperature electric signal. This renders the values of the temperature during the vibration experiments useless. Thus an indirect method needs to be used to estimate the temperature of the bulk fluid.

Figure 3 shows the evolution of the interface as the cell is heated from a subcritical temperature (T_c − 45 mK) towards T_c at a very slow rate (20 mK/min) for a= 0.83 mm, f= 35 Hz, and gravity level $0.05g_0$. The interface looks fuzzy, due to the effect of vibrations. What is indeed observed is the position of an interface that exhibits periodic oscillations in phase with the exciting vibration around its mean, steady-state position. Figure 3(a) shows the interface attaining a dynamic equilibrium, tilting towards the right wall. In our experiments the interface always seemed to tilt towards the right wall. This nonrandom behavior is presumably due to a slight initial tilt in the cell with respect to the vibrational direction (as can be seen in Fig. 2). In the absence of this initial tilt, the interface should randomly choose a particular wall based on the experimental perturbations. It is not supposed to flip to the other wall once it has found its equilibrium position.

As the temperature of the cell is further increased, the interface deforms giving rise to the so-called frozen wave instability [6]. Figure 3(b) shows the transition region when the tilted interface destabilizes, giving birth to the frozen waves [Figs. 3(c) and 3(d)]. See the Supplemental Material [18] explaining the evolution of the interface as the temperature is varied for the case $a = 0.83$ mm, $f = 35$ Hz, and $g = 0.05g_0$.

Experiments and subsequent analysis of the frozen wave instability (treated in Ref. [19]) have shown that the wavelength (λ) of the frozen wave instability depends on the thermal proximity to the critical point $\Delta T (= T_c - T)$ according to the empirical relation

$$\lambda = S\frac{\Delta T^{0.38}}{g^{0.8}}(a\omega)^{1.2}. \quad (9)$$

Here S is a proportionality constant that depends on the working fluid. For H_2, $S = 0.075$ with all the quantities in SI units. The temperature of the bulk fluid can be estimated by first calculating the temperature for a particular wavelength of the frozen wave instability and then extrapolating it using the fact that the heating of the cell is carried out at approximately 20 mK min^{-1}. This method, although approximate, is sufficient for the present analysis.

B. Phenomenological understanding of the tilting of the interface

It is well known that when a liquid filled in a reservoir is subjected to a constant acceleration $\vec{a_0}$, the interface of the liquid tilts at an angle α given by $\tan(\alpha) = (g + a_{0y})/a_{0x}$ with respect to the vertical. This is due to the fact that the interface aligns perpendicular to the direction of the effective gravity. Though this phenomenon is a little bit different from the phenomenon observed in our experiments, they share the same root as will be demonstrated below.

The tilting of the liquid-vapor interface in our experiments is caused by the nonlinear interaction of vibration with the interface. This happens when a threshold vibrational acceleration is exceeded. Lyubimov and Cherepanov [4] analytically treated the frozen wave problem involving two incompressible inviscid fluids subjected to horizontal

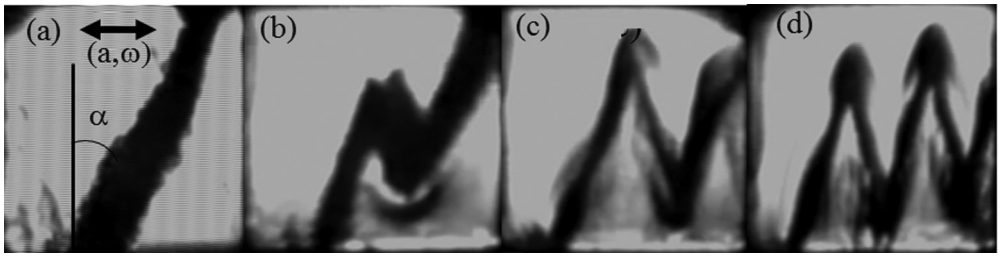

FIG. 3. Evolution of the dynamics at the interface for the vibration case $a = 0.83$ mm, $f = 35$ Hz, and gravity level $0.05g_0$ as the temperature is increased from approximately T_c−45 mK (a) to T_c−15 mK (d) .

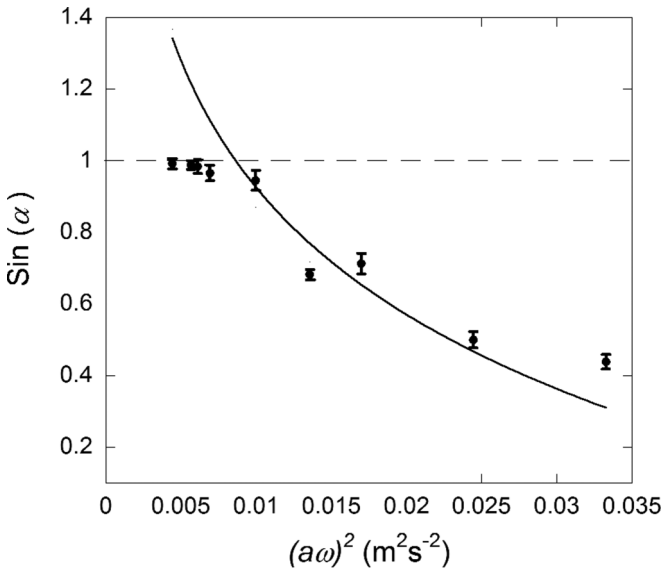

FIG. 4. Comparison of the experimental results with theory ($g = 0.05g_0$).

vibration. Their approach involved, under high-frequency approximation ($\Omega = \omega h^2/\nu \gg 1$), the splitting of the equations of motion into pulsating and average parts. A supplementary assumption of low amplitude ($a/h \ll 1$) allows linearizing the pulsating fields and solving them separately. For the present experiments, Ω lies between 3000 and 15 000 while a/h lies between 0.1 and 0.01, showing that we are in the validity range of the Lyubimov and Cherepanov theory. The resulting averaged equations using the standard notation are reproduced from [4] as below:

$$du_\beta/dt = -\nabla p_\beta/\rho_\beta + \nu_\beta \Delta u_\beta - \left[g\vec{\gamma} + \nabla\left((a\omega)^2 V_\beta^2\right)\right], \quad (10)$$

where u_β is the averaged velocity field, V_β is the relative amplitude (with respect to $a\omega$) of the pulsating velocity field, $\vec{\gamma}$ is the unit vector indicating the direction of the acceleration due to gravity, and the subscript β refers to the two fluids.

Equation (10) along with the relevant boundary conditions can be solved to obtain the average flow field of the problem. Such an analysis is, however, out of the scope of the present paper. Our interest in discussing the above equation is merely to explain the phenomenology of the tilted interface. As can be seen from Eq. (10), the pulsating velocity fields induce an extra acceleration term $\nabla((a\omega)^2 V_\beta^2)$ in the average flow field of the problem. The averaged equations indicated by Eq. (10) are phenomenologically similar to a fluid filled inside a square cavity subjected to a constant acceleration equal to $\overrightarrow{a_0} = \nabla((a\omega)^2 V_\beta^2)$. The nature of this acceleration term needs to be determined by appropriate analytical methods to compare it to Eq. (8), which is not taken up in the present paper.

C. Effect of vibrational parameters on the angle of the interface

From the temperature of the bulk fluid estimated according to the procedure described in the previous section, theoretical values of $\sin\alpha$ can be calculated by using Eq. (8). The results of the experiments are compared with the theory in Fig. 4 for gravity acceleration $0.05g_0$ and for various values of amplitudes and frequencies. The solid dots in the plot are the results of the experiments for various values of $a^2\omega^2$. The solid line is derived from Eq. (8) for the corresponding values of $a^2\omega^2$.

The following observations can be made. When the vibrational velocity is increased, the angle of the interface with respect to the vertical decreases. For smaller values of $a\omega$, the interface remains relatively horizontal ($\sin\alpha \sim 1$). It can be seen that Eq. (8) compares well with the experiments for smaller values of α. The dispersion in the experimental values is attributed to errors in the calculation of the temperature values and errors in the measurement of the angle of the interface. However, an exact agreement with Eq. (8) cannot be expected due to the approximation made in the equation [as we already mentioned in the Introduction, Eq. (8) is valid for small angles of α (large values of $a\omega$)]. The experiments carried out using the gravity level $0.01g_0$, however, do not match very well with Eq. (8) due to the fact that the uniformity of the gravity field itself is of the order of $0.025g_0$, which is much higher than the gravity sought.

It is important to note that the observed tilted interface cannot be an incomplete frozen wave. By comparing the results of Fig. 4 with Eq. (9), the wavelength of a frozen wave is seen to increase with $a\omega$ whereas the angular tilt of the interface with respect to the vertical (angle α) decreases as $a\omega$ is increased. In fact, the frozen waves grow from the tilted interface when the conditions corresponding to the instability threshold are met [Fig. 3(b)].

D. Effect of thermal proximity on the angle of the interface

As has been mentioned earlier, as one approaches the critical point, various properties of a near-critical fluid vary with the proximity to the critical point according to universal

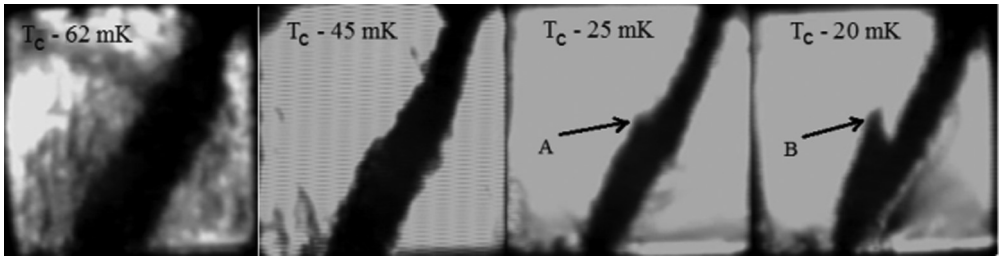

FIG. 5. Effect of $T_c - T$ on the angle of the interface when the temperature of the cell is changed from $T_c - 62$ mK to $T_c - 20$ mK for the vibration case $a = 0.83$ mm, $f = 35$ Hz, and gravity level $0.05g_0$. A and B indicate the start of frozen waves instabilities (see text).

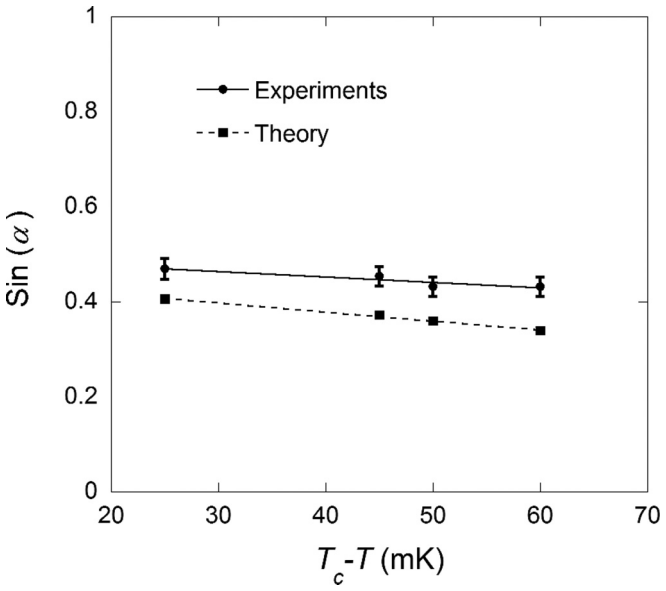

FIG. 6. Effect of $(T_c - T)$ on the angle of the interface (comparison with theory).

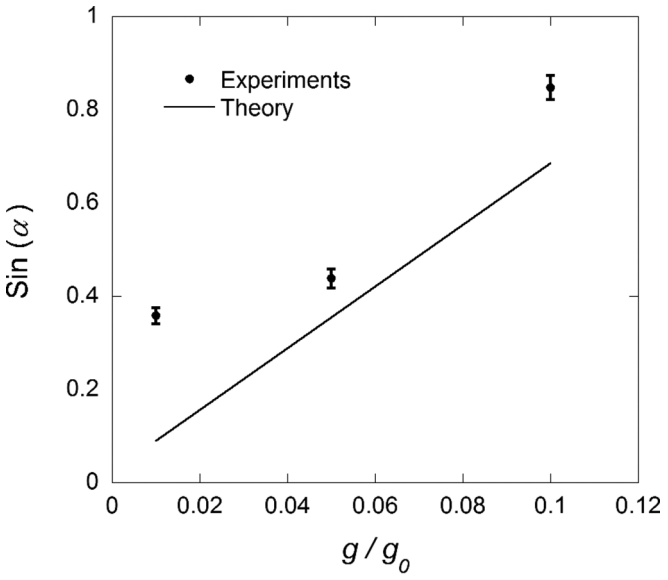

FIG. 8. Effect of g on the angle of the interface for $a = 0.83$ mm and $f = 35$ Hz.

scaled power laws [13]. Thus, studying the effect of the temperature on the angle of the interface is an important aspect of the problem. Figure 5 presents the results of experiments for the case $a = 0.83$ mm, $f = 35$ Hz, and $g = 0.05g_0$. In the pictures presented, the temperature of the cell changes from $T_c - 62$ mK to $T_c - 20$ mK. It can be seen that the angle of the interface does not change much between $T_c - 62$ mK and $T_c - 25$ mK. A small bump is already evident on the interface (shown as "A" in Fig. 5) at $T_c - 25$ mK. which indicates the nascence of the frozen waves. They develop much more at $T_c - 20$ mK (shown as "B" in Fig. 5).

Equation (8) describes the dependence of the angle of the interface on the relative density ratio $(\rho_l + \rho_v)/(\rho_l - \rho_v)$. The liquid-vapor density difference $\Delta\rho(= \rho_l - \rho_v)$ varies with $\varepsilon = (T_c - T)/T_c$, the relative critical point proximity, according to [13]:

$$\Delta\rho = 2B\rho_c\varepsilon^{0.325}. \tag{11}$$

The values of $(\rho_l + \rho_v)/(\rho_l - \rho_v)$ are calculated for various temperatures using data from NIST [20] and from Eq. (11) and are then used to calculate the theoretical values of $\sin\alpha$ from Eq. (8). Figure 6 shows the effect of critical point proximity $(T_c - T)$ on the angle of the interface and compares the results of the experiments with theory. It can be observed from the plot that as the fluid approaches the critical point, the angle of the interface increases. In the range of the temperatures considered, drastic change in the angle of the interface is not seen because the values of $(\rho_l + \rho_v)/(\rho_l - \rho_v)$ change only by $\pm 7\%$ with respect to the median temperature. Comparison of the results of the experiments and theory show good agreement. It can be seen that the trend of the plots is the same.

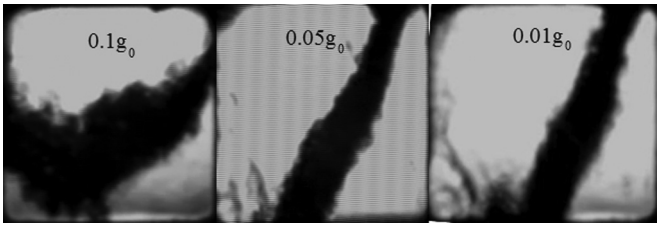

FIG. 7. Effect of g on the angle of the interface with respect to gravity field for $a = 0.83$ mm and $f = 35$ Hz.

E. Effect of vibrational parameters on the angle of the interface

Figure 7 shows the images of the interface corresponding to the vibration case $a = 0.83$ mm and $f = 35$ Hz for various gravity levels $0.1g_0, 0.05g_0$, and $0.01g_0$. It can be seen that as the gravity is reduced, the angle of the interface reduces, well in agreement with Eq. (8).

Figure 8 compares the results of the experiments with theory. The solid dots are the experimental results while the solid line traces Eq. (8). It can be seen that the general trend of the plots is the same. The point corresponding to $0.01g_0$ deviates considerably from the line. This is due to the fact that the uniformity of the gravity levels inside the cell is of the order of $0.025g_0$, greater than the gravity level sought.

IV. CONCLUSION

Vibration experiments were carried out on a liquid-vapor interface of H_2 to study the dynamic equilibrium of the interface. The study was performed for various combinations of amplitude and frequency of vibration and for various gravity levels, thanks to the magnetic gravity compensation instrument HYLDE. Experiments showed that under harmonic vibrations the equilibrium position of an interface can considerably deviate from its normally horizontal position and attain large enough angles. When compared with the theoretical correlation derived by Wolf [5], the data compared well with theory, although this latter suffers from substantial approximation.

It is interesting to note that under vanishing gravity, vibration acts on an interface in the same way as an artificial gravity. Further theoretical work seems to be desirable to deepen our understanding of this phenomenon.

ACKNOWLEDGMENTS

The authors gratefully acknowledge financial support from the CNES (France) and financial support from the Government of Perm Region, Russia (Contract No. C-26/212).

[1] M. Faraday, Philos. Trans. R. Soc. London **52**, 299 (1831).
[2] T. B. Benjamin and F. Ursell, Proc. R. Soc. London, Ser. A **225**, 505 (1954).
[3] J. Porter, I. Tinao, A. Laveron-Simavilla, and C. A. Lopez, Fluid Dyn. Res. **44**, 065501 (2012).
[4] D. V. Lyubimov and A. A. Cherepanov, Fluid Dyn. **21**, 849 (1987).
[5] G. H. Wolf, Z. Phys. B **227**, 291 (1969).
[6] R. Wunenburger, P. Evesque, C. Chabot, Y. Garrabos, S. Fauve, and D. Beysens, Phys. Rev. E **59**, 5440 (1999).
[7] E. Talib, S. V. Jalikop, and A. Juel, J. Fluid Mech. **584**, 45 (2007).
[8] http://en.wikipedia.org/wiki/Kapitza's_pendulum
[9] P. L. Kapitza, Sov. Phys. JETP **21**, 588 (1951).
[10] L. D. Landau and E. M. Lifschitz, *Mechanics* (Mir, Moscow, 1973).
[11] E. I. Butikov, Am. J. Phys. **69**, 755 (2001).
[12] D. V. Lyubimov, T. P. Lyubimova, and A. A. Cherapanov, *Dynamics of Fluid Interfaces in Vibrational Fields* (Fizmatlit, Moscow, 2003) (in Russian).
[13] B. Zappoli, D. Beysens, and Y. Garrabos, *Heat Transfers and Related Effects in Supercritical Fluids* (Springer, New-York/Heidelberg) (in press).
[14] R.Wunenburger, D. Chatain, Y. Garrabos, and D. Beysens, Phys. Rev. E **62**, 469 (2000).
[15] D. Chatain, D. Beysens, K. Madet, V. Nikolayev, and A. Mailfert, Microgravity Sci. Technol. **18**, 196 (2006).
[16] L. Quettier, H. Felice, A. Mailfert, D. Chatain, and D. Beysens, Eur. Phys. J. Appl. Phys. **32**, 167 (2005).
[17] C. Morteau, M. Salzmann, Y. Garrabos, and D. Beysens, in *Proceedings of the Second European Symposium on Fluids in Space, Neaple, Italy, 22–26 April 1996*, edited by A. Viviani (Edizioni Jean Gilder Congressi srl, Neaple, 1996), pp. 327–333.
[18] See Supplemental Material at http://link.aps.org/supplemental/10.1103/PhysRevE.89.063003 for video clip of evolution of the interface for the case $a = 0.83$ mm, $f = 35$ Hz, $g = 0.05g_0$.
[19] G. Gandikota, D. Chatain, S. Amiroudine, T. Lyubimova, and D. Beysens, Phys. Rev. E **89**, 012309 (2014).
[20] NIST Chemistry WebBook (http://webbook.nist.gov/chemistry/fluid/).